

Direct atomic flux measurement of electron-beam evaporated yttrium with a diode-laser-based atomic absorption monitor at 668 nm

Weizhi Wang,^{a)} R. H. Hammond, M. M. Fejer, S. Arnason, and M. R. Beasley
Edward L. Ginzton Laboratory, Stanford University, Stanford, California 94305

M. L. Bortz^{b)} and T. Day
Focused Research, Inc., Santa Clara, California 95051

(Received 20 January 1997; accepted for publication 6 May 1997)

A direct measurement of atomic flux in *e*-beam evaporated yttrium has been demonstrated with a diode-laser-based atomic absorption (AA) monitor at 668 nm. Atomic number density and velocity were measured through absorption and Doppler shift measurements to provide the atomic flux. The AA-based deposition rates were compared with independent quartz crystal monitors showing agreement between the two methods. © 1997 American Institute of Physics.
[S0003-6951(97)03527-4]

Most industrial thin film syntheses use measurement of the deposition rate for controlling the deposition process. Conventional methods for measuring the deposition rate, e.g., quartz crystal monitors (QCM), cannot always meet the requirements for advanced applications such as composition control in the deposition of compounds and alloys, where element-specific monitors are desirable. Vapor sensing based on laser spectroscopy techniques is attractive for such applications. Sensors based on highly coherent lasers have advantages with respect to both conventional monitors and hollow cathode lamp based spectroscopic monitors, e.g., they are simultaneously both element specific and noninvasive; they can measure the atomic flux, which contains information on both density and velocity, rather than a simple density, for precise process control and study of the deposition process; the integration and interface of multiple element-specific systems with the vacuum chamber is easy. Furthermore, the tunability of the laser enables the measurement of optically thick vapors. The only extra requirement compared to conventional monitors is the optical access windows in the deposition chamber.

We have previously developed diode-laser-based atomic absorption (AA) monitors for atomic density measurements in the visible¹ and the blue-UV region.² In this letter, we demonstrate simultaneous measurement of the atomic density and velocity, and thus the atomic flux in an *e*-beam evaporated yttrium system with a diode-laser-based monitor. For material systems with near-unity sticking coefficients, control of this vapor flux allows direct control of the film deposition rate.

The atomic flux Γ is defined as $\Gamma = n\nu$, and the relationship between Γ and the deposition rate $R[\text{\AA}/\text{s}]$ is $R = km\Gamma/\rho$, where k is the sticking coefficient, m is the atomic mass, n is the atomic number density, ν is the mean velocity of the atoms, and ρ is the density of the deposited film. In yttrium deposition, the sticking coefficient is approximately equal to unity. Thus, we can calculate the deposition rate from the atomic flux obtained from the atomic density and velocity with the AA monitor.

The diode-laser-based AA monitor incorporated an external cavity diode laser (ECDL) operating at 668 nm, corresponding to a ground state absorption of yttrium. Laser radiation was delivered to the chamber by a single-mode polarization-maintaining fiber, and laser radiation was received from the chamber and directed to the sensor using a 400- μm -core multimode fiber, providing versatility in configuring either a single- or a double-pass mode of operation, as shown in Figs. 1(a) and 1(b).

The spectroscopic technique, based on wavelength modulation spectroscopy and autobalanced detection, allows for high sensitivity, wide dynamic range, and low drift using simple electronics and requires a minimum number of components. Wavelength modulation at 1.2 kHz was achieved by dithering the piezoelectric tuning element within the external cavity laser; demodulation using a lock-in amplifier results in an output signal proportional to the first derivative of the absorption lineshape. Throughout these experiments, the center frequency of the laser was scanned at rates around 1–10 Hz over a range of about 5 GHz centered on the ab-

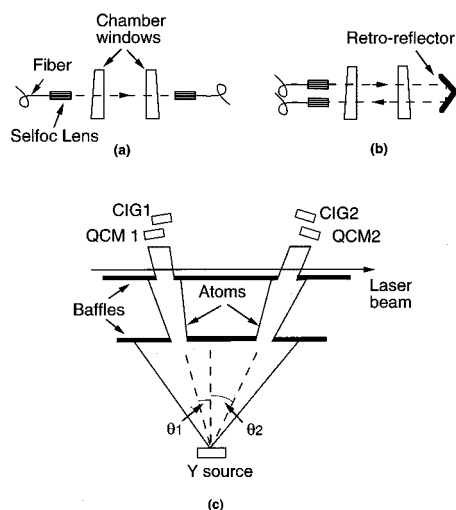


FIG. 1. (a) Single-pass mode and (b) double-pass mode. (c) Experimental configuration inside the *e*-beam evaporation chamber. QCM 1 and 2 are quartz crystal monitors. CIG 1 and 2 are chopped ion gauges for feedback control. Two baffles were used for collimating the atomic beam. The two QCMs were placed with their surfaces normal to the atomic beams.

^{a)}Electronic mail: wwang@loki.stanford.edu

^{b)}Present address: SDL, Inc., 80 Rose Orchard Way, San Jose, CA 94134.

sorption line, to recover the entire absorption line.

The ECDL has an excess noise of >20 dB above the shot noise limit at low frequencies (several kHz), and has significant amplitude variations while being tuned. In a wavelength modulation scheme, this amplitude variation translates into residual amplitude modulation at the modulation frequency. To reduce these effects, an autobalanced detection system was employed.³ The detector has both reference and signal photodiodes, and the output is automatically balanced by a feedback loop in the detection circuit so as to maintain optimum operation despite unequal signal and reference powers. The detector also provides an output proportional to the power of the signal channel that can be used to normalize changes in the system transmission due to contamination of chamber windows, variations of coupling efficiencies of optical devices, etc. The combination of autobalanced detection and wavelength modulation reduced baseline artifacts in the spectroscopic technique to a typical level equivalent to an absorption of 10^{-5} . The dominant source of the instrumental uncertainty was the uncorrected etalon fringes caused by reflections from the optical surfaces in the system.

To model the sensor performance, the atomic density is assumed to be uniform over the path length for simplicity. The signal from the lock-in amplifier normalized by the dc output from the signal channel can be expressed as $S = G a l \alpha'(\nu)$, where G is the combined gain of the lock-in amplifier and the detector, a is the amplitude of the frequency dither, l is the path length, and $\alpha'(\nu)$ is the first derivative of the absorption coefficient. Since the area J under the absorption curve $J = \int \alpha(\nu) d\nu = \lambda^2 A n / 8\pi$, where λ is the wavelength and A is the Einstein spontaneous emission coefficient of the excited state, the atomic density can be calculated by integrating the normalized derivative signal as $n = 8\pi J / [G(a/\delta\nu)\lambda^2 A l]$, where $\delta\nu$ is the frequency step for integration.

In order to measure the velocity of the atoms, two baffles for spatially filtering the atomic vapor into two beams angled with respect to the laser beam were installed as shown in Fig. 1(c). The Doppler shifts (DS) of the center frequency of the absorption line, determined by the velocity of the atoms and the geometry of the apparatus, were measured for obtaining the velocity. In the current experiment, the relative DS of the two beams was obtained by measuring the frequency separation of the line centers of the two atomic beams without using any additional frequency reference. The mean velocity of the atoms can be expressed as $\nu = 2\pi^{-1/2} D S \lambda / (\sin \theta_1 + \sin \theta_2)$, assuming that the atoms are evaporated from a point source with a velocity distribution independent of θ , where θ_1 and θ_2 are angles shown in Fig. 1(c).

Yttrium has a nuclear spin of $1/2$ resulting in magnetic-dipole-induced hyperfine splittings in both the ground and excited states. Figure 2 shows the hyperfine structure and the intensity ratio of these splittings. In our experiment, the hyperfine splittings were partially resolved. Figure 3(a) shows a typical lineshape obtained by integrating the derivative signal, for a case where only one of the two openings in the baffle was opened. The broadening of each line is due to the residual Doppler broadening arising from the finite size of the baffle opening and the tilt angle between the laser beam

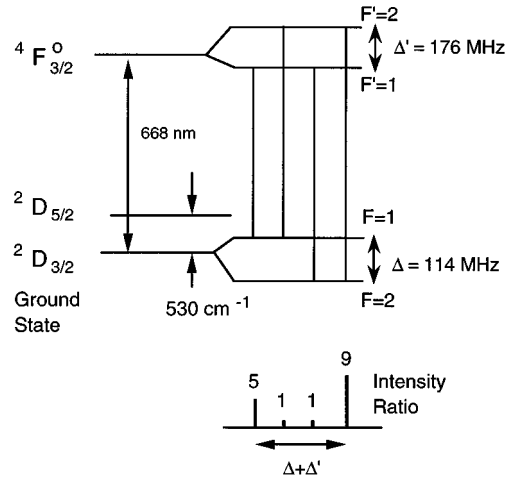


FIG. 2. Energy levels illustrating hyperfine structures in both ground and excited states, and the theoretical intensity ratios of these splittings. The hyperfine splitting constant for the ground state is -57.2 MHz, and the constant for the excited state in our experiment is 88 MHz. The hyperfine splittings are twice the hyperfine constants.

and the atomic beam. Assuming that each hyperfine component has a Gaussian lineshape with the same width, each component can be characterized by an absorption magnitude α_0 and a width $\Delta\nu$, i.e., $\alpha_0 \exp[-(\Omega/\Delta\nu)^2]$, where Ω is the frequency detuning from the resonance. By curve-fitting with the known hyperfine constant for the ground state (-57.2 MHz),⁴ and the ratios of the relative intensities,⁵ the hyperfine splitting constant of $4F_{3/2}^0$ level was measured to be 88 MHz.

All measurements in the present experiment were performed with a laser intensity well below the saturation intensity. Otherwise, reduced absorption due to saturation will be encountered. The saturation intensity was measured to be ~ 2 mW/cm² in the present e -beam evaporation experiment for the 668 nm transition.

Figure 3(b) shows the lineshape obtained in single-pass mode with both openings in the baffle uncovered. The two sets of hyperfine lines were Doppler-shifted relative to one another but partially overlap since the Doppler shift was comparable to the hyperfine splitting. Although the area un-

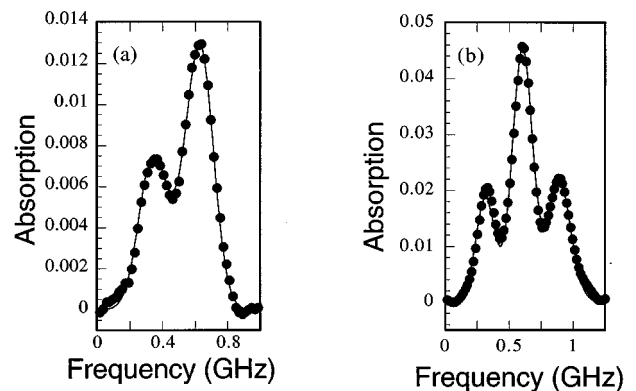


FIG. 3. (a) A typical lineshape of absorption in single-pass mode with one opening in the baffle, showing the hyperfine splittings. (b) Absorption lineshape when two openings in the baffle, showing superposition of Doppler-shifted profiles of the two atomic beams. The solid lines are fitted curves.

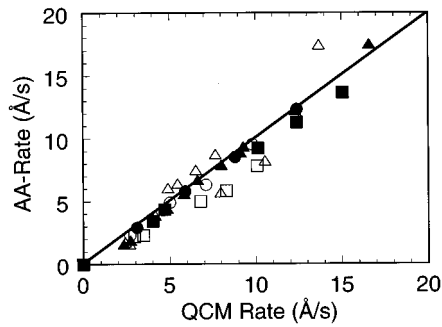


FIG. 4. Measured relationship between the QCM rates and the rates from AA monitor. Solid and open symbols represent R_1 and R_2 measured by AA for atomic beams 1 and 2, and are plotted vs rates from QCM1 and QCM2, respectively. Different shapes represent different runs. Note significantly better agreement for data from atomic beam 1.

der the absorption curve is independent of the broadening mechanism, in order to separate the contributions to the absorption from the two atomic beams, and to measure the Doppler shift, curve fitting was performed assuming a Gaussian lineshape for each component. The same Doppler linewidth was assumed for all hyperfine components of each atomic beam, but different Doppler widths were allowed for the two beams.

It should be noted that the atomic number density of yttrium measured by the absorption in the AA monitor corresponded to the $^2D_{3/2} \rightarrow ^4F_{3/2}^0$ transition. There is another energy level ($^2D_{5/2}$) with an energy $\Delta E = 530 \text{ cm}^{-1}$ above the ground state ($^2D_{3/2}$) (see Fig. 2), which has significant thermal occupation at the temperatures characteristic of the evaporation process. The equilibrium ratio of the ground state population to the total population is equal to $r = [1 + (3/2)\exp(-\Delta E/k_B T)]^{-1}$, where $3/2$ is the degeneracy ratio of the two levels, T is the temperature, and k_B is the Boltzmann constant.

Combining the absorption and Doppler measurements, the deposition rate in each beam was calculated according to

$$R_i = \frac{16\pi^{1/2} m J_i D S}{r \rho l A \lambda G (a/\delta\nu) (\sin \theta_1 + \sin \theta_2)},$$

where $m = 1.48 \times 10^{-22} \text{ g}$, $\rho = 4.34 \text{ g/cm}^3$, $l = 4.2 \text{ cm}$, $\lambda = 668 \text{ nm}$, $A = 4.8 \times 10^5 \text{ s}^{-1}$,⁶ $G = 650$, $a = 35 \text{ MHz}$, $\delta\nu = 20 \text{ MHz}$, $\theta_1 = 1.5^\circ$, and $\theta_2 = 13^\circ$; R_i and J_i ($i = 1, 2$) are the rates and the areas under absorption curves for the atomic beams, respectively. The actual atomic density was corrected to the QCM rate by using a population ratio factor $r = 0.48$, which corresponds to a temperature of 2300 K. Figure 4 shows the measured relationship between the QCM rate and the deposition rate based on AA measurement. From the result obtained in three independent runs, R_1 agreed well with the QCM rates while R_2 scattered around the QCM rates, especially at higher rates.

The deviations in the data were larger than the instrumental uncertainty. Two uncertainties in the physical model of the atomic flux measurement in the e -beam evaporation are considered as the probable source of the discrepancy. One is the population of the metastable level. Noticing that R_2 corresponds to the opening with the larger tilt angle, the spatially anisotropic scattering of the evaporated atoms in a

nonthermal-equilibrium evaporation process may result in spatial-temporal variations both in the ratio of the velocity components perpendicular and parallel to the laser beam, and in the metastable population factor r , rendering inadequate the approximation of a single constant value for these factors. Another is that the point source model is oversimplified. These two factors may result in a larger deviation in the presence of a high background pressure. Observations in the experiments suggest that a more precise model of the ‘‘virtual source’’⁷ of the nonthermal-equilibrium e -beam evaporation process is needed.

To solve these problems, alternative configurations with less model sensitivity are being considered. Simultaneous measurements of both the ground state and the metastable levels in yttrium with two lasers (668 and 679 nm) is under investigation. A scheme with two optical beams counter-propagating at an angle to the substrate surface, can directly measure the normal component of the velocity. Preliminary experiments in such a geometry, measuring e -beam evaporated barium (which in addition has no low-lying metastable levels), indicate a pressure-independent result.

For thin film deposition applications, the atomic flux should be derived without using a particular aperture. Because of the complicated line-integrated absorption profile associated with the velocity and number density distributions, modeling of the evaporation process is a key problem and a current research focus. Diode-laser-based AA monitor provides a powerful tool to acquire sufficient information for this purpose. It should be pointed out that for reactive deposition, monitors must also operate at a relatively high background pressure ($10^{-5} - 10^{-4}$ Torr). The AA sensing is useful because the oxidation occurs only on the substrate at this pressure range, so that the flux of the atoms rather than their oxides is still the target to control.

In summary, we have demonstrated a direct measurement of the atomic flux in e -beam evaporated yttrium using a diode-laser-based atomic absorption (AA) monitor at 668 nm. The atomic number density and velocity were measured through absorption and Doppler shift measurements. The AA-based rates were compared with independent quartz crystal monitors, showing agreement between the methods. Issues related to process-dependent population of the metastable level and azimuthal asymmetry of the velocity distribution are under investigation.

This project is supported by ARPA through Conductus and ONR N00014-94-C-0197.

¹W. Wang, R. H. Hammond, M. M. Fejer, C. H. Ahn, M. R. Beasley, M. D. Levenson, and M. L. Bortz, *Appl. Phys. Lett.* **67**, 1375 (1995).

²W. Wang, M. M. Fejer, R. H. Hammond, M. R. Beasley, C. H. Ahn, M. L. Bortz, and T. Day, *Appl. Phys. Lett.* **68**, 729 (1996).

³P. C. D. Hobbs, *Opt. Photonics News*, (April), 17 (1991).

⁴A. A. Radzig and B. M. Smirnov, *Springer Series in Chemical Physics* (Springer, Berlin, 1980), Vol. 31, p. 102.

⁵H. E. White and A. Y. Eliason, *Phys. Rev.* **44**, 753 (1933).

⁶C. H. Corliss and W. R. Bozman, *NBS Spec. Publ.* **53**, 527 (1962).

⁷M. D. Miller, P. J. Bilotto, and M. Benapfl, *J. Vac. Sci. Technol. A* **11**, 2851 (1993).